IOP Publishing Journal of Physics D: Applied Physics
J. Phys. D: Appl. Phys. **40** (2007) 2759–2764 doi:10.1088/0022-3727/40/9/013

A single-gap transflective fringe field switching display using a liquid crystal with positive dielectric anisotropy

Young Jin Lim[1], **Myong-Hoon Lee**[1], **Gi-Dong Lee**[2], **Won-Gun Jang**[3] **and Seung Hee Lee**[1]

[1] BK-21 Polymer BIN Fusion Research Team, Research Center for Advanced Materials Development, School of Advanced Materials Engineering, Chonbuk National University, Chonju, Chonbuk 561-756, Korea
[2] Department of Electronics Engineering, Dong-A University, Pusan 607-735, Korea
[3] Korea Photonics Technology Institute, Wolchul-dong, Buk-gu, Gwangju, 500-460, Korea

E-mail: gdlee@dau.ac.kr (GDL) and lsh1@chonbuk.ac.kr (SHL)

Received 12 December 2006, in final form 13 March 2007
Published 19 April 2007
Online at stacks.iop.org/JPhysD/40/2759

Abstract
There is considerable difficulty in fabricating a reflector with embossing in an array substrate using a conventional single gap transflective fringe-field switching nematic liquid-crystal display. In order to solve this problem, we propose a new structure, which consists of a reflector on a colour filter substrate. The newly proposed structure with a complex field direction has problems such that the voltage-dependent transmittance and reflectance curves do not match each other, which necessitate a dual driving circuit. This paper reports the optimized electrode structure and calculated electro-optical results realizing a single gamma curve and high light efficiency.

1. Introduction

Transflective liquid-crystal displays (LCDs) have been developed for portable electronic devices because of their quality visibility under many environmental lighting conditions whilst maintaining their beneficial characteristics such as portability, good legibility and low power consumption [1]. Recently, a single-cell-gap transflective display associated with the fringe-field switching (FFS) mode was proposed, which uses a LC with negative dielectric anisotropy [2, 3]. However, the rotation angle of the LC director in the transmissive region is double that in the reflective part, causing mismatch in the voltage-dependence between the transmittance (T) and reflectance (R) curves. Since then, many new structures using both types of LC with negative (−LC) and positive (+LC) dielectric anisotropy have been proposed to produce a competitive product with a single gamma and embossed reflector [4–6]. In the normal FFS mode, the pixel and common electrodes are formed only on one (array) substrate in the form of slits and planes, respectively. Hence, the formation of a reflector with embossing is quite difficult [7]. Constructing the reflector on a colour filter (CF) substrate is also possible but this alters the fringe-field direction and electro-optic characteristics of the device, particularly when using +LC.

This paper proposes a new cell structure for a transflective FFS display using +LC with a high image quality and a single driving circuit as well as a single cell gap, which simplifies the process of fabricating the reflector with embossing. The detailed electro-optic characteristics are described.

2. Cell structure and switching principle

Figure 1 shows a cross-sectional and top view of the proposed single-cell-gap transflective associated with a FFS device. This device differs from conventional FFS transflective devices [3, 6] in that the pixel and the common electrodes exist only on the top substrate with a thin-film transistor. The pixel electrode is patterned with an electrode width (w) and distance (l') between them and has a slant angle of α with respect to the horizontal rubbing direction in the transmissive and reflective parts. The reflector exists only in the reflective part on the bottom substrate, which may be electrically connected to the common electrode on the top substrate. An in-cell retarder exists above the reflector. Since the +LC, which orients parallel

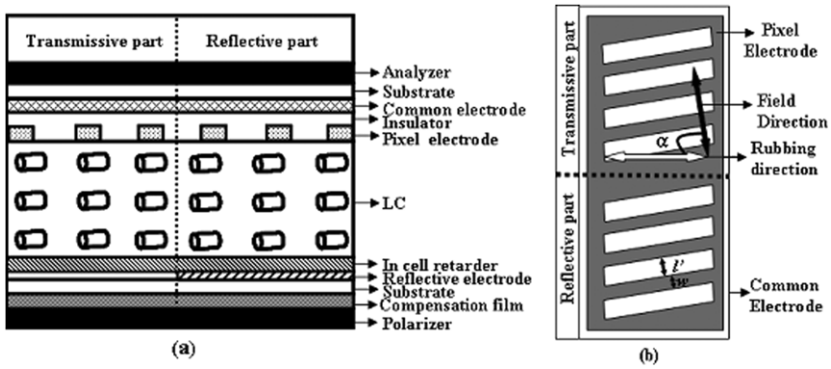

Figure 1. Electrode structure of the transflective display using FFS mode: (*a*) cross-section and (*b*) top view.

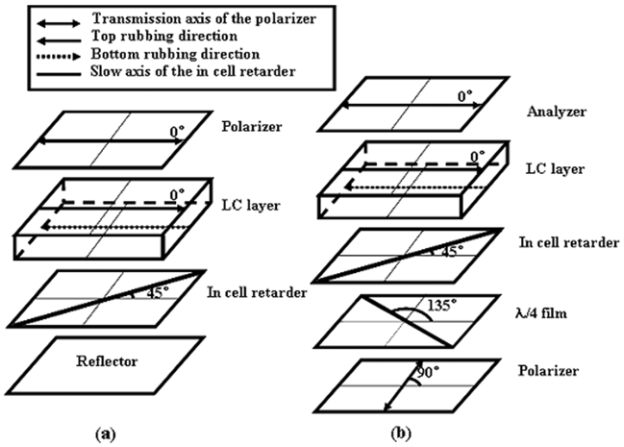

Figure 2. Optical configurations of the optical layers in the device: (*a*) reflective and (*b*) transmissive part.

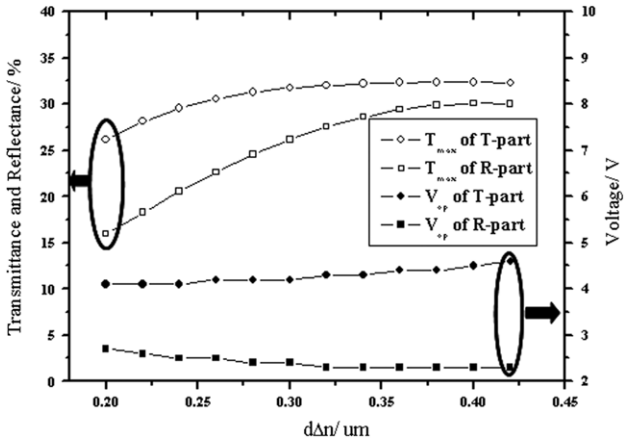

Figure 3. Maximum R, T and operation voltages of each part as a function of $d\Delta n$.

to the field direction, is used and the reflective electrode is connected to the common electrode of the top substrate, the field distribution is strongly affected by the reflector in that a strong vertical field is generated between the pixel and the common electrodes. This vertical field will cause the +LC to tilt upwards instead of twisting, which would result in a low R due to insufficient twisting.

Figure 2 shows the optical configuration of the proposed single gap transflective LCD, which is similar to the one previously reported with the −LC [3]. The in-cell retarder with a quarter-wave (λ/4) plate exists above the patterned reflector and its optic axis makes a 45° angle with respect to the analyser. Another λ/4 plate exists between the bottom substrate and the polarizer with its optic axis orthogonal to the in-cell retarder. The cell retardation value was used to generate a phase change of λ/2 when a fringe-electric field was applied homogeneously to the aligned LC director whose optic axis is coincident with the analyser. The polarizers cross each other. In this way, R and T are zero at the voltage-off state as $\Psi = 0^\circ$ because R and T are proportional to $\sin^2(4\Psi)$ and $\sin^2(2\Psi)$, respectively, where Ψ is the angle between the crossed polarizers and the LC director. The bright state is achieved when a voltage is applied to rotate the LC director by 22.5° and 45° in the reflective and transmissive parts, respectively.

A horizontal electric field is required to rotate the LC director in plane. However, the existence of a common electrode on the bottom (reflector) and top substrate increases the vertical field intensity between the pixel electrode on the top substrate and the common electrode on the bottom substrate. Therefore, although a rotation angle of only 22.5° is needed in the reflective part, it is difficult to induce adequate rotation of the LC. The existence of a reflector is inevitable necessitating a decrease in vertical field intensity. In our proposed cell structure, there is an overcoat layer with a thickness of 2 μm, which is essential for planarization of the CF, and an in-cell retarder with a thickness of 1 μm above the reflector. The multi-dielectric layers decrease the vertical field intensity between the pixel and the common electrodes. Therefore, the LC director can be twisted to some degree rather than just tilted upwards. In this way, the LC director can rotate by 22.5°, giving rise to a good R.

3. Simulation condition and optimal cell retardation to maximize light efficiency

The overcoat above the reflector was not considered in the first calculation. In order to maximize R and T, the effective LC cell retardation value should be λ/2. Interestingly, in the FFS mode, the maximal reflectance ($R_{\max}$) and transmittance ($T_{\max}$) are dependent on the electrode position, i.e. oscillating along the electrode position because the horizontal field intensity rotating the LC changes periodically along the electrode positions [8, 9]. Therefore, the average values of $R_{\max}$ and

T_{max} along the electrodes were calculated as a function of $d\Delta n$, while changing Δn at a fixed cell gap of 4 μm, as shown in figure 3. The LCD master (Shintech, Japan) was used for the calculations. An electrode structure with an electrode width of 3 μm and a distance of 4.5 μm between the electrodes was considered. LCs with physical parameters such as dielectric anisotropy $\Delta\varepsilon = 7.4$, and elastic constants $K_1 = 11.7$ pN, $K_2 = 5.1$ pN and $K_3 = 16.1$ pN were used, and the surface tilt angle of the LC was 2° with an angle, α, of 80° with respect to the horizontal component of the fringe-electric field. A 2×2 extended Jones matrix was used to calculate R and T [10]. The transmittances for the single and parallel polarizers were assumed to be 41% and 35%, respectively.

As indicated in figure 3, T increased from 26% to 32% as the $d\Delta n$ of the LC increased from 0.20 to 0.42 μm , and R increased from 16% to 30% as the $d\Delta n$ increased from 0.20 to 0.42 μm . In addition, the operating voltage (V_{op}) of the reflective part decreases slightly from 2.7 to 2.3 V. However, the V_{op} for the transmissive part increases slightly from 4.1 to 4.6 V when the $d\Delta n$ is increased from 0.2 to 0.42 μm. The difference in the V_{op} between the transmissive and reflective parts is due to the difference in the rotating angle of the LC director in the white state. With the exception of the difference in the V_{op}, the device has a relatively wide margin in cell retardation value because the white state and V_{op} do not change as rapidly as the $d\Delta n$ of the LC. In addition, the dark state of the device in the normal direction is insensitive to variations in $d\Delta n$, which is required in real cell fabrication for mass production. In this study, 0.40 μm was chosen as the cell retardation value considering the maximization of the light efficiency and low V_{op}.

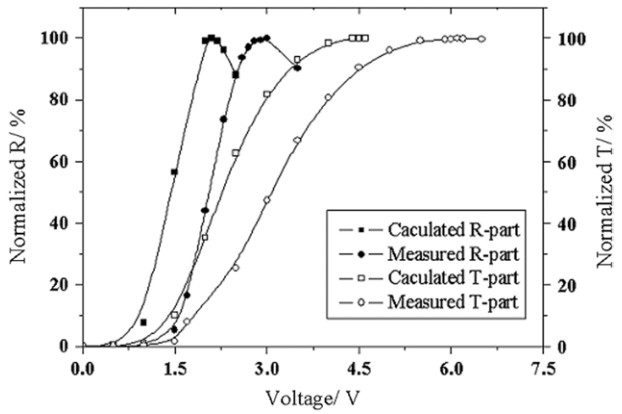

Figure 4. Calculated and measured voltage-dependent $R$and T curves.

4. Optimized cell structure and results

With these chosen cell parameters and a dielectric layer above the reflector, the voltage-dependent normalized R (V–R) and T (V–T) were calculated and measured, as shown in figure 4. As expected, the calculated and measured R and T curves do not coincide. The V_{op} in the reflective part was approximately half of that in the transmissive part. Here, the V–R and V–T curves between the calculation and the experimental results do not match precisely even though they showed a similar trend. It was found that the calculation results always showed a lower V_{op} than the measured one, which might have been due to differences in defining the surface anchoring energy, the size of the electrode structure and the thickness and dielectric constant of each layer.

In order to achieve a single gamma curve, it was realized that the electrode structure of the reflective part in the array substrate and α should be changed, as suggested elsewhere [4–6]. The transflective cell structure was revised to achieve a better performance, as shown in figure 5. The cell structure in the transmissive part was the same as before. However, the cell structure in the reflective part was changed in that the plane shape of the common electrode was patterned into slit forms and there is some distance (l) between the pixel and the common electrodes and the electrode width of the pixel and the common electrodes. With this change in structure, the LC is driven mainly by the horizontal field rather than by the fringe field in the reflective region. An overcoat above the reflector with an embossing pattern is used to remove the image parallax. The R, as a function of the insulation thickness, was calculated and the result showed that if the insulation thickness is increased to 3 μm (here we assume the dielectric constant of the layer to be 3), R reaches approximately the same as that in the normal FFS without the electrode on the opposite

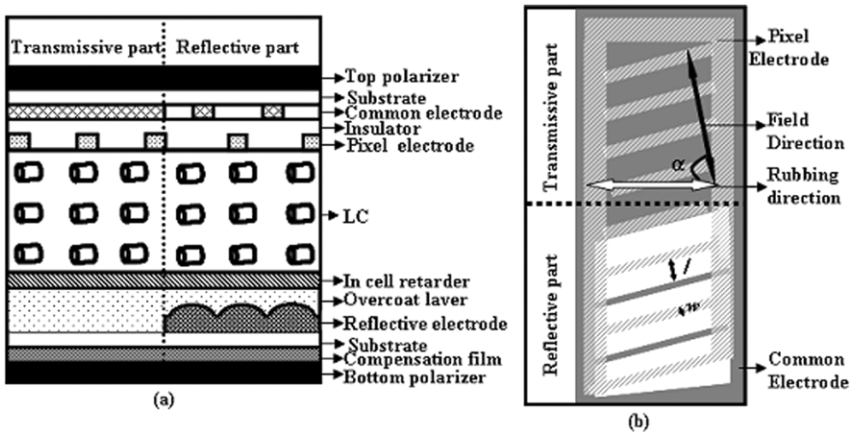

Figure 5. Cell structure of the new transflective FFS display: (*a*) cross-section and (*b*) top view.

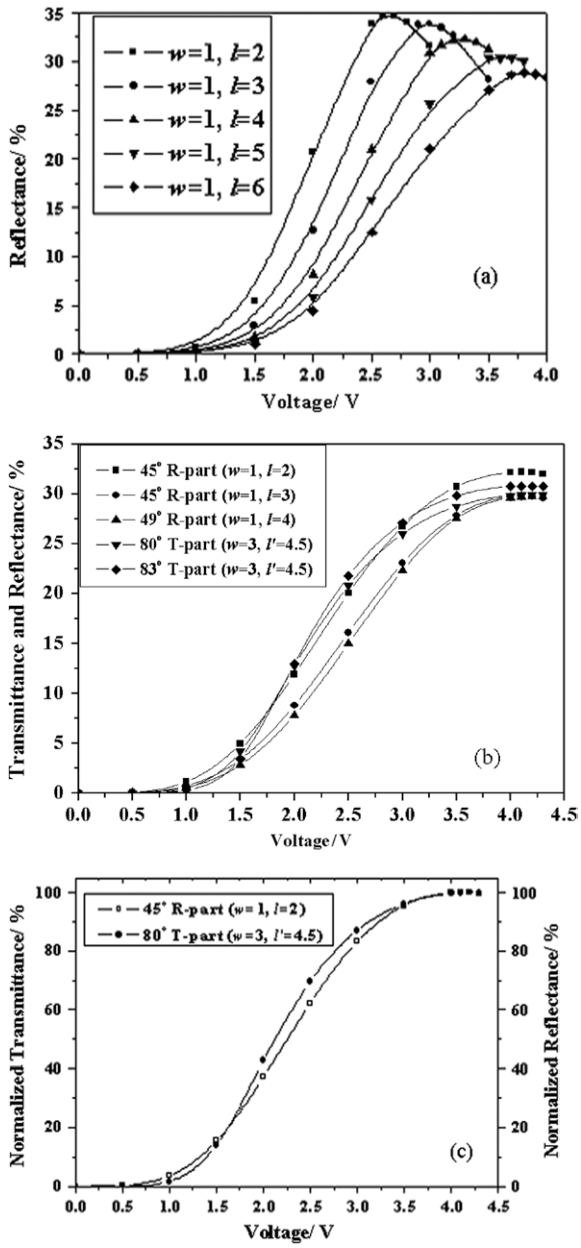

Figure 6. Voltage-dependent (*a*) R curves for various electrode widths, (*b*) R and T curves for various rubbing angles and (*c*) normalized T and R curves in the optimum.

side of the array substrate [11]. In a real situation, several insulation layers such as CF, overcoat and in-cell retarder with a total thickness $>3\,\mu$m can exist above the reflector. Hence, a high R can be achieved with this structure.

The voltage-dependent R curves were calculated as a function of l at a fixed electrode width, where α was assumed to be 80° with respect to the horizontal field and the insulation thickness was $3\,\mu$m, as shown in figure 6(*a*). The V–R can be expected to change with varying electrode structure. The results show that the $V_{\rm op}$ increases and the reflectance drops with increasing l. However, R decreases with increasing l until $l = 5\,\mu$m, and the rate of decrease in reflectance is not excessive, compared with that of the previous transflective FFS mode [11]. Therefore, the electrode structure was changed

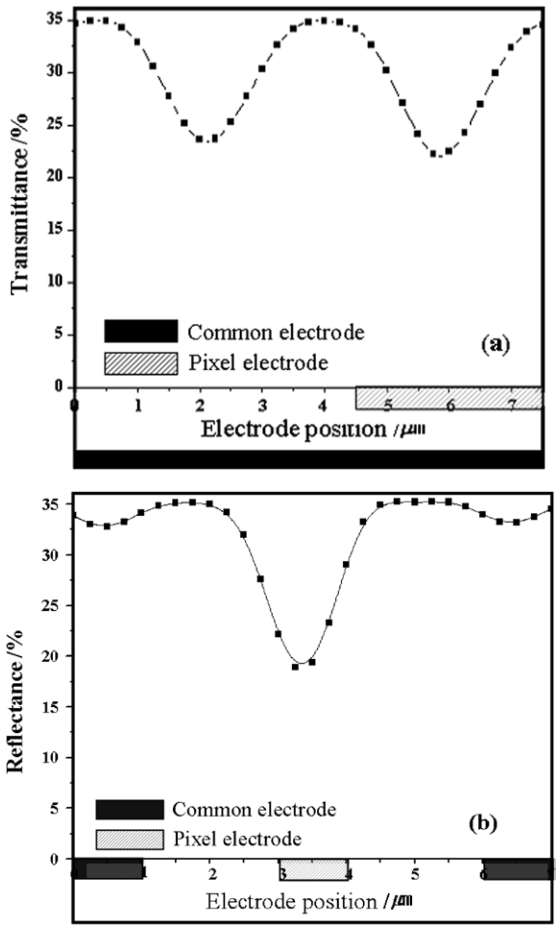

Figure 7. T and R distribution along the electrode position at operating voltages in (*a*) transmissive and (*b*) reflective parts.

by $l = 5\,\mu$m for the reflective region, and the rubbing angle (or slit angle of electrode) was optimized in both reflective and transmissive regions because the V–R curve is also strongly dependent on the rubbing angle with respect to the horizontal field [5, 6]. Figure 6(*b*) shows the calculated V–R and V–T curves as a function of the rubbing angles and electrode structure in the reflective and transmissive areas. In the reflective area, the $V_{\rm op}$ increases sharply with decreasing rubbing angle. From these results, optimized V–R and V–T curves that are approximately coincident with each other could be achieved, as shown in figure 6(*c*). The $V_{\rm op}$ were 4.1 and 4.2 V in the reflective and transmissive parts, when the rubbing angles were 45° and 80°, respectively.

Figure 7 shows how T and R vary along the electrode position in the optimized condition. In the transmissive part, T is the highest at both edges of the electrodes and the lowest at the centre of the pixel and the common electrodes, respectively, which correlates with the different twist angles of the LC director along the electrodes. In the reflective part, R is the lowest at the centre of the pixel due to the existence of a vertical field between the reflective electrode on the bottom and the pixel on top, resulting from insufficient twist angle of the LC director in that part. Nevertheless, the whole R is similar to the total T because R is very high between the pixel and the common electrodes and above the common electrode.

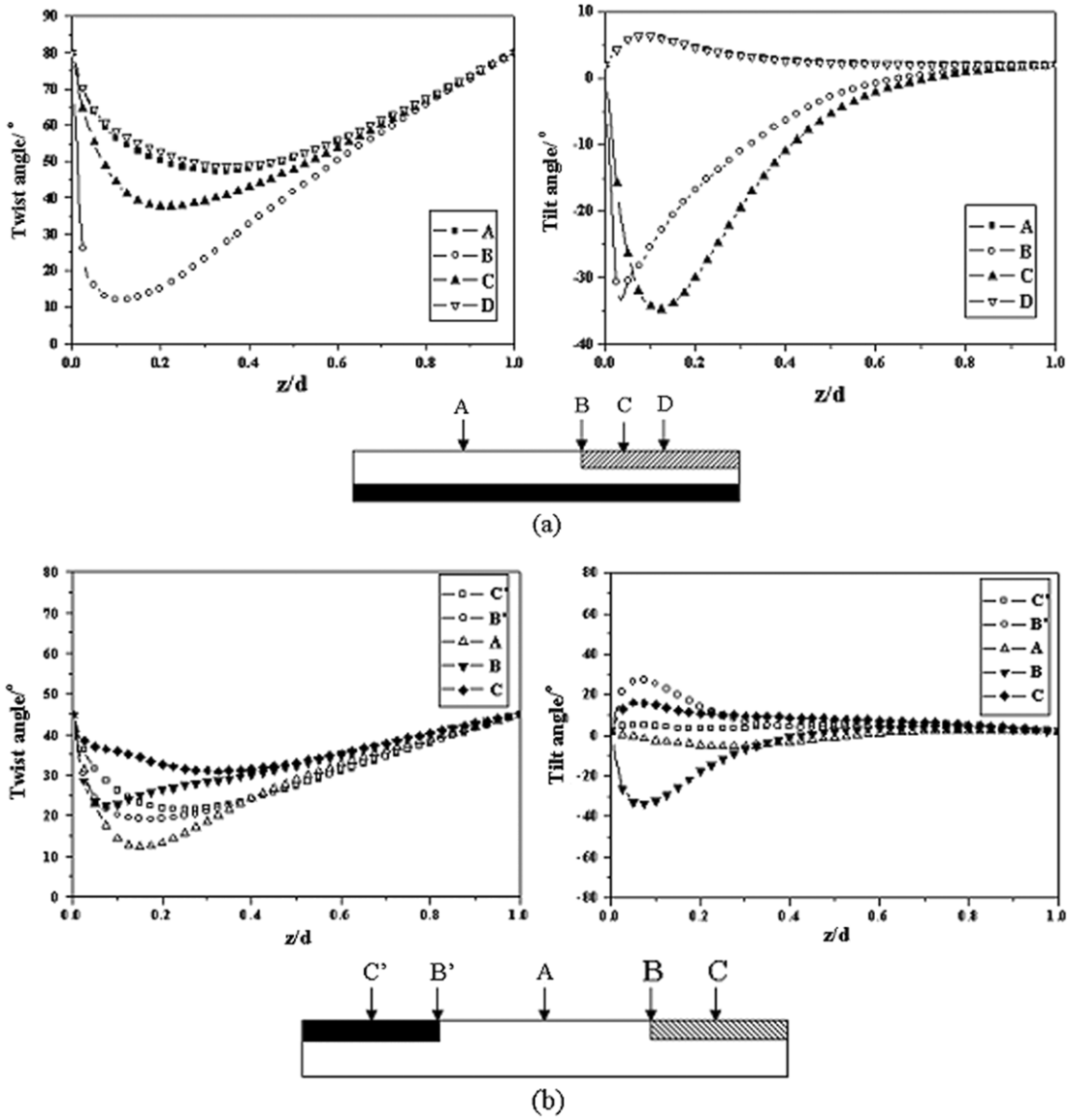

Figure 8. LC orientation at the different electrode positions in the (*a*) transmissive and (*b*) reflective parts.

Figure 8 shows the calculated LC orientation in a white state at several different electrode positions when using a LC with positive dielectric anisotropy. In the transmissive part, the LC orientation is strongly dependent on the electrode position such that the maximum twist angle of the LC director with respect to the rubbing direction of 80° at the centre of electrode (A and D) at $z/d = 0.325$ is only 32° (it is obtained by $80° - 48°$) due to the high tilt angle generated at the electrode position (C) between the edge (B) and centre, while it was 68° ($= 80° - 12°$) at $z/d = 0.1$ at electrode position B. As expected, this difference in twist angle causes an oscillating T along the electrodes. In the reflective part, which has a very narrow electrode width and distance, R above the pixel electrode and common electrode was asymmetrical due to the existence of a vertical field between the pixel and reflective electrode and the lack of potential difference between the reflective and common electrodes. Consequently, when investigating the LC orientation in detail in the reflective part, the maximum tilt angle 32° (at $z/d = 0.075$) at B is much higher than the 25° (at $z/d = 0.075$) at B′. This results in a lower twist angle at position C (average twist angle = 8.5° with respect to initial rubbing angle of 45°) than that (14°) at position C′ (see figure 8(*b*)), which clearly shows a low R at position C.

Finally, the viewing angle characteristics were calculated. Figure 9 shows the iso-contrast contour at an incident wavelength of 550 nm in the single gap transflective display. In the transmissive part, there is a region at which the CR is $>5:1$ to a polar angle of almost 80° in all directions. Even in the reflective part, this region exists in most directions to a polar angle of almost 80° except for a certain azimuthal direction. The CR of the device is better than in-plane switching and multi-domain vertical alignment modes with a wide viewing angle [12].

5. Summary

This study examined a single-gap and −gamma transflective FFS display with an optimized cell structure. In this device, the reflector exists on the opposite side of the array substrate,

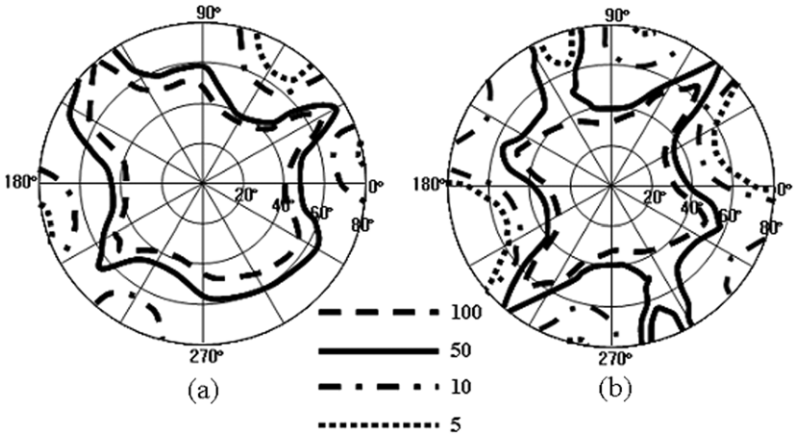

Figure 9. Iso-contrast contours at an incident wavelength of 550 nm in the single gap transflective display using positive LC: (*a*) transmissive and (*b*) reflective parts.

which allows a rather easy fabrication process to form an embossing reflector on the CF substrate. The electrode structure and rubbing angle were optimized and a single-gap and −gamma transflective FFS display showed a wide viewing angle. However, the device still requires an in-cell retarder, which is a difficult process in LCDs. Therefore, more study will be needed to achieve a higher performance and low cost transflective FFS display.

Acknowledgment

This work was supported by Grant No R01-2004-000-10014-0 from the Basic Research Program of the Korea Science & Engineering Foundation.

References

[1] Watanabe R and Tomita O 2002 *Proc. 9th Int. Display Workshops (Hiroshima)* p 397
[2] Song J H, Lim Y J, Park C H and Lee S H 2004 *Proc. KIEEME Ann. Autumn Conf. (Chungwoon University)* p 567
[3] Song J H, Lim Y J, Lee M-H, LEE S H and Shin S T 2005 *Appl. Phys. Lett.* **87** 011108
[4] Jeong Y H, Kim H Y, Park J B, Kim M S, Kim G H, Seen S M, Lim D H, Kim S Y, Lim Y J and Lee S H 2005 *SID'05 Digest (Boston, MA)* p 723
[5] Park J B, Kim H Y, Jeong Y H, Lim D H, Kim S Y and Lim Y J 2005 *Japan. J. App. Phys.* **44** 6701
[6] Lim Y J, Jeong Y H, Choi M O, Jang W G and Lee S H 2005 *Japan. J. Appl. Phys.* **44** L1532
[7] Song J H, Lim D H, Park J B, Kim M S, Jeong Y H, Kim H Y, Kim S Y, Lim Y J and Lee S H 2005 *Proc. 12th Int. Display Workshops (Takamatsu)* p 103
[8] Kim S J, Kim H Y, Lee S H, Lee Y K, Park K C and Jang J 2005 *Japan. J. Appl. Phys.* **44** 6581
[9] Jung S H, Kim H Y, Lee M-H, Rhee J M and Lee S H 2005 *Liq. Cryst.* **32** 267
[10] Lien A 1990 *Appl. Phys. Lett.* **57** 2767
[11] Choi M O, Song J H, Lim Y J, Kim T H and Lee S H 2005 *SID'05 Digest (Boston, MA)* p 719
[12] Zhu X, Ge Z and Wu S T 2006 *J. Displ. Tech.* **2** 2